31st International Conference
ENGINEERING MECHANICS 2025
Medlov, Czech Republic, May 12 –14, 2025
Paper **#63,** pp. 225–228, doi: 10.21495/em2025-225

MECHANICAL PROPERTIES OF POWDER-BED 3D PRINTED CONCRETE FOR LIGHTWEIGHT CONSTRUCTION ELEMENTS

Hlaváček P.[1], Wolf C.[2], Robens-Rademacher A.[3], Kühne H.-C.[4]

Abstract: *This work focuses on developing the 3D printing process of concrete using powder bed technology, with an emphasis on the mechanical properties of the printed samples. Parallelly, a topology optimization strategy is applied to reduce the material needed for the customized production of structurally complex lightweight construction elements. The powder bed technology ensures almost complete freedom of shaping with the loss-free use of dry mortar powder, making the optimized design practically feasible. Optimization of material and technology for 3D powder bed printing is discussed in terms of overall porosity, bulk density and wettability of the powder used, as well as the technology of powder bed recoating and the amount of activator solution. The strength of printed samples for handling, shape accuracy and final strength after hardening are considered as governing parameters for the material and process development.*

Keywords: Concrete, powder-bed 3D print, mechanical properties, topology optimization

1. Introduction

In the construction sector, there is a huge potential for innovative solutions that reduce material need while maintaining properties and functionality of the structure. This study addresses this approach by developing and applying powder bed technology for the additive manufacturing of optimized lightweight concrete components. By combining numerical methods for designing customized building elements with 3D manufacturing technology, the study aims to achieve efficient resource utilization in both the design and printing processes. A key objective is to advance and establish powder bed manufacturing technology, making its advantages and potential for cement-bound materials practically applicable.

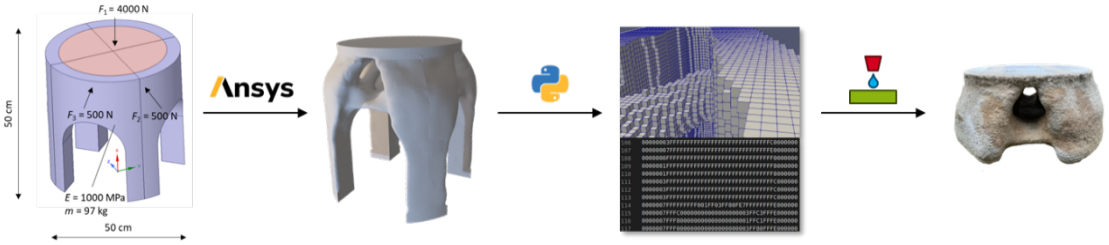

Fig. 1: Workflow for comprehensive processing of a structure from design/modelling to 3D print.

[1] Ing. Petr Hlaváček, Ph.D.: Bundesanstalt für Materialforschung und -prüfung (BAM), 7.4 Technology of construction materials; Unter den Eichen 87; 12205, Berlin; Germany, petr.hlavacek@bam.de

[2] Christoph Wolf, M.Sc.: Bundesanstalt für Materialforschung und -prüfung (BAM), 7.7 Modelling and Simulation; Unter den Eichen 87; 12205, Berlin; Germany, christoph.wolf@bam.de

[3] Dr. Annika Robens-Radermacher: Bundesanstalt für Materialforschung und -prüfung (BAM), 7.7 Modelling and Simulation; Unter den Eichen 87; 12205, Berlin; Germany, annika.robens-radermacher@bam.de

[4] Dr.-Ing. Hans-Carsten Kühne: Bundesanstalt für Materialforschung und -prüfung (BAM), 7.4 Technology of construction materials; Unter den Eichen 87; 12205, Berlin; Germany, hans-carsten.kuehne@bam.de

2. Material for 3D print

The powder-bed print technology for cementitious materials needs a rapid hardening binders to ensure effectivity of the print process and acceptable resolution of the printed bodies as presented *e.g.* by Hlaváček et al. (2024). Recently, a phosphate cement binder was utilized by Salari et al. (2024) for conducting a comprehensive study on process parameters and their effect on compressive strength of the 3D printed bodies. In this work, the 3D print mortar is based on fast hardening cement Fastcrete® from Schwenk, Germany, blended with quartz sand from Ottendorf-Okrilla and additives improving the print resolution and stability. The composition of the mortar is as given in Table 1. The w/c ratio is determined by the amount of water injected into the powder bed during the print process and varies between 0.3 and 0.5. A lower w/c ratio is critical due to poor connection between adjacent voxels, while a higher ratio can result in samples with poorer geometric accuracy.

Tab. 1: Composition of the 3D print mortar for powder bed technology, mass in kg per 1m³.

Cement	Ottendorf-Okrilla sand			
Fastcrete®	0.1-0.3 mm	0.1-0.5 mm	0.5-1.0 mm	Additives
404,7	303,6	303,6	607,2	2,0

3. Topology optimization

The topology optimization approach, which starts from geometry input and ends with 3D printing instructions has been formulated and offers fast and reliable results for different architectural inputs with minimal user interaction needs. The input geometry is optimized to reduce mass and CO_2 emissions based on a geometric model of the global design (given as a standard STL file) and defined load cases. The constraints for topology optimization are as presented by Wolf et al. (2024): stress constraints (mitigating tension and limiting compressive stress using Drucker-Prager based models), geometric constraints (preserving specific surfaces from material removal during optimization), and manufacturing constraints (controlling member size and avoiding trapped powder in inclusions without connection to the outside). The topology optimization problem is formulated using SIMP method (Solid Isotropic Material with Penalization, simplest form) with following governing equations as derived *e.g.* in (Bendsøe and Sigmund, 2004) and presented by Wolf et al. (2024):

Mass and/or compliance minimization using weights w_M and w_C:

$$M = \int_\Omega \bar{\rho}\mathrm{d}\Omega \quad \text{and} \quad C = \int_\Omega \boldsymbol{\varepsilon}(\mathbf{u}) E(\bar{\rho}) \boldsymbol{\varepsilon}(\mathbf{u}) \mathrm{d}\Omega \tag{1}$$
$$\min_{\rho} \quad w_M M + w_C C \quad \text{and} \quad 0 \leq \rho \leq 1; \quad w_M, w_C \geq 0$$

Displacement (u) based weak form of linear elasticity problem:

$$\text{s.t.} \quad \int_\Omega E(\bar{\rho}) \boldsymbol{s}(\mathbf{u}) \cdot \nabla \tilde{\mathbf{u}} \, \mathrm{d}\Omega = \int_\Omega \boldsymbol{b} \cdot \tilde{\mathbf{u}} \, \mathrm{d}\Omega + \int_{\Gamma_t} \boldsymbol{t} \cdot \tilde{\mathbf{u}} \, \mathrm{d}\Gamma, \quad \forall \tilde{\mathbf{u}} \in \tilde{V} \tag{2}$$

Stress constraints for every element e:

$$\begin{aligned} \sigma_{\mathrm{Mises,e}} &\leq \sigma_{\mathrm{Mises,lim}}, \ \forall \mathrm{e} \\ \sigma_{1,\mathrm{e}} &\leq \sigma_{1,\mathrm{lim}}, \ \forall \mathrm{e} \end{aligned} \tag{3}$$

and finally, the SIMP approach within unit Youngs modulus E:

$$\boldsymbol{\sigma}(\mathbf{u}) = E(\bar{\rho}) \boldsymbol{s}(\mathbf{u}) \quad \text{with} \quad E(\bar{\rho}) = E_{\min} + (E_0 - E_{\min}) \bar{\rho}^q \tag{4}$$

The process receives input from upstream material tests, providing insights into strength, stiffness, and possible anisotropy. This integration of material testing enhances the accuracy and reliability of the optimization, aligning the design with the real-world behavior of 3D printed concrete. An important aspect of the workflow is the segmentation of the optimized global structure into substructures, aligning with the size limitations of the 3D powder-bed printer.

4. Results

The compressive strength, flexural strength and *E* modulus of the 3D-printed concrete in powder bed were determined from tests on standard 40x40x160 mm specimens autoclaved at 185°C for 24 hours for faster strength gain after printing. To ensure flat surface for inserting specimens into the jaws of the testing device, the specimens were cut to target size on diamond saw prior to testing. Figure 2 shows a typical stress-strain diagram for three-point bending test of the 3D-printed concrete with a highlighted linear elastic part and linear fit for determination of *E* modulus.

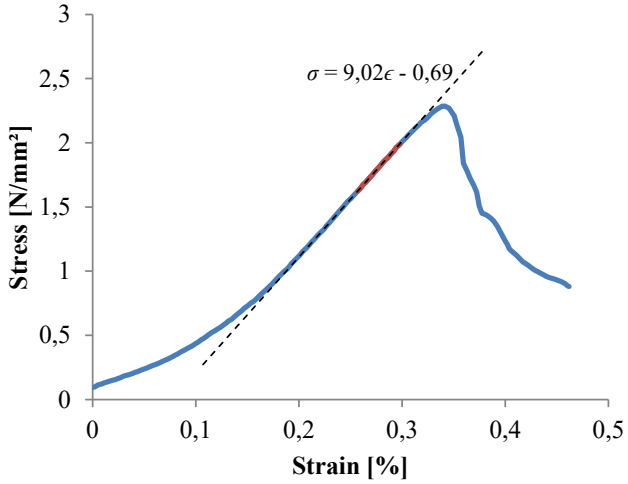

Fig. 2: Typical stress-strain diagram for three-point bending test of the 3D-printed concrete.

The compressive strength of the 3D printed mortar from Table 1 after hardening is approximately 12 MPa and flexural strength 2,5 MPa for a w/c ratio of 0.35 when printed into a directly deposited powder bed. The main factor contributing to the relatively low strength is the high porosity (approx. 40%) in the deposited powder bed (ρ_{bulk} 1,65 g/cm³). To reduce the porosity and increase strength, the powder bed can be compacted prior to 3D print process. Compacting the powder bed prior to 3D printing can present challenges with the penetration of the activator into the powder bed, which in turn prolongs the 3D printing process and makes it harder for the activator to penetrate evenly. Thus, an optimal density is sought to balance final strength and process efficiency. By compacting the powder bed to achieve a total porosity of around 25% (ρ_{bulk} 2,0 g/cm³), the compressive strength of the 3D printed parts after hardening increases to approximately 21 MPa and flexural strength to 4 MPa.

Table 2 shows the input parameters and results for a topology optimization example of the structure given in Figure 1. The results for the four parameter sets are visualized in Figure 3.

Tab. 2: Examples of topology optimization with four different input parameters.

Design *nr.*	①	②	③	④
Element size (avg) [mm]	10	21	10	10
Obj. Function weights w_M and w_C [-]	$w_M = 1$, $w_C = 0$	$w_M = 1$, $w_C = 0$	$w_M = 1$, $w_C = 1$	$w_M = 1$, $w_C = 0$
$\sigma_{Mises,lim}$ [Mpa]	0.50	0.50	0.50	1.00
$\sigma_{1,lim}$ [Mpa]	0.55	0.55	0.55	0.55
Mass [kg]	30.0	44.3	58.1	22.8
$\sigma_{Mises,max}$ [Mpa]	0.44	0.47	0.37	0.87
$\sigma_{1,min}$ [Mpa]	0.51	0.48	0.40	0.55

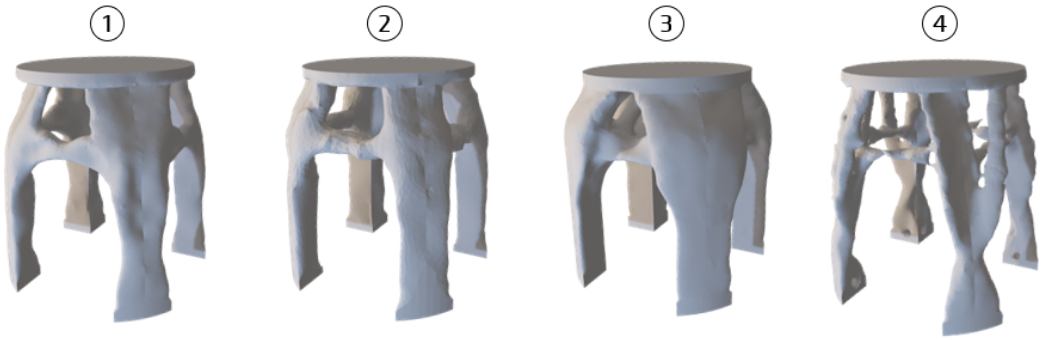

Fig. 3: Visualization of the results of the topology optimization task based on four different input parameter sets as given in Table 2.

5. Conclusions

Powder bed technology is an excellent method for implementing topology-optimized structures due to its ability to build almost without geometrical constraints. The only limiting factor is that the printed part must be depowdered after the print finishes. This means the printed part must be removed from the unbound powder, so there cannot be hollow closed spaces in the structure where the unbound powder would remain. To ensure proper handling strength during the depowdering process, a rapid hardening binder is to be used. For the final strength after hardening, the overall porosity of the concrete, resulting from the bulk density of the applied powder bed, has been identified as a critical parameter. An optimal degree of powder compaction was found to ensure proper water penetration into the powder bed while maintaining feasible mechanical properties of the 3D printed material.

The topology optimization example demonstrates the holistic approach to design 3D printed concrete structures. By integrating material parameters, structural experiments, and fabrication considerations into the optimization process, it is possible to achieve designs that are not only structurally optimized but also practical to fabricate and maintains required performance characteristics.

Acknowledgement

The authors gratefully acknowledge the support of this work by the Technologietransfer-Programm Leichtbau (TTP LB) of the German Federal Ministry for Economic Affairs and Climate Action (Bundesministerium für Wirtschaft und Klimaschutz, BMWK) under the project SupLeichtAF.

References

Bendsøe, M. P. and Sigmund, O. (2004). Topology Optimization: Theory, Methods, and Applications. Springer.

Hlaváček, P., Diercks, P., Robens-Radermacher, A. and Kühne, H.-C. (2024). Powder-bed 3D printing of cementitious materials for lightweight construction elements. Presented at the 4th RILEM International Conference on Concrete and Digital Fabrication (Digital Concrete 2024), Munich, Germany.

Salari, F., Zocca, A., Bosetti, P., Hlaváček, P., Italiano, A., Gobbin, F., Colombo, P., Kühne, H.-C. and Sglavo, V. M. (2024). Powder-bed 3D printing by selective activation of magnesium phosphate cement: Determining significant processing parameters and their effect on mechanical strength. Open Ceramics.

Wolf, C., Robens-Radermacher, A. and Unger, J. F. (2024). Optimization framework for powder bed 3D printed concrete structures under various constraints. Presented at the 4th RILEM International Conference on Concrete and Digital Fabrication (Digital Concrete 2024), Munich, Germany.